SUPPLEMENTARY INFORMATION

An unusual cobalt(II)-based single-walled metal−organic nanotube

Tien-Wen Tseng,*[a] Tzuoo-Tsair Luo,[b] Chong-Cheng Su,[a,b] Hui-Huan Hsu,[a,b] Chen-I Yang,*[c] and Kuang-Lieh Lu*[b]

[a]Department of Chemical Engineering, National Taipei University of Technology, Taipei 106, Taiwan
[b]Institute of Chemistry, Academia Sinica, Taipei 115, Taiwan
[c]Department of Chemistry, Tunghai University, Taichung 242, Taiwan

Contents

(a) (b)

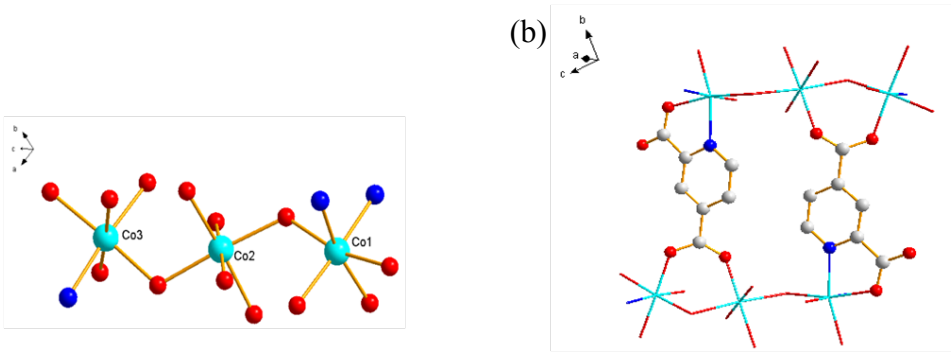

Fig. S1 (a) The trinuclear cluster of **1** possesses three types of cobalt(II) (Co1, Co2, and Co3) ions linking via an oxygen atom from 2,4-pydc^{2-} ligand. (b) The cluster units are connected by the 2,4-pydc^{2-} ligand, which acts as a linker.

(a) (b)

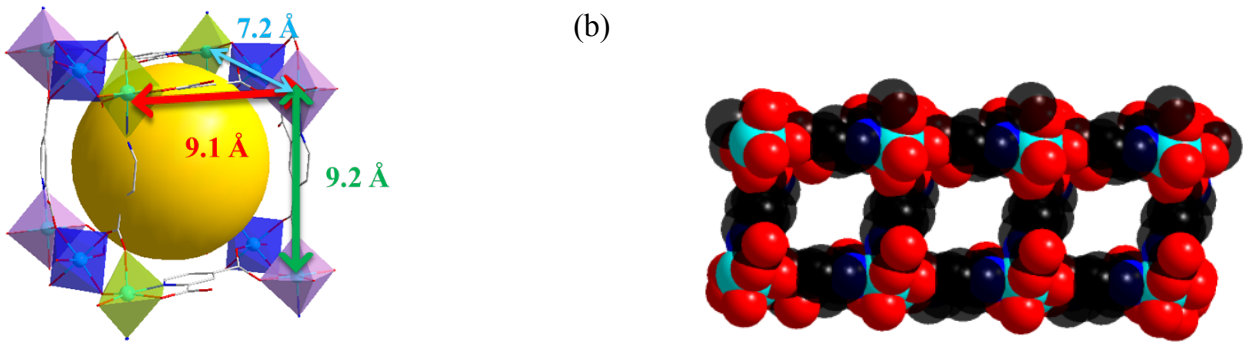

Fig. S2 The structures of **1**: (a) the structural building unit has a box-like with dimensions of 7.2 × 9.1 × 9.2 Å^3 (highlighted in yellow color), that is constructed by four cluster units and eight 2,4-pydc^{2-} ligands. (b) the channel size is estimated to be 13.8 × 11.8 Å^2, which was substracted by the van der Waals radii of atoms.

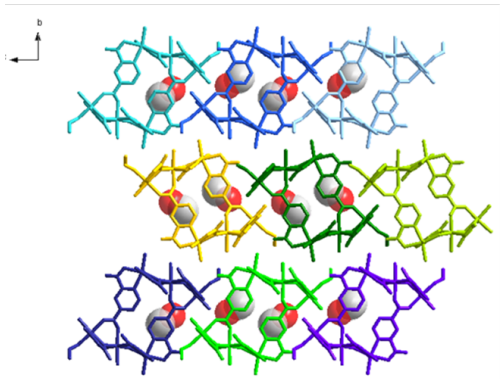

Fig. S3 One ethanol molecule is included within each box of **1** (oxygen in red and carbon in grey) viewed along the *a* axis.

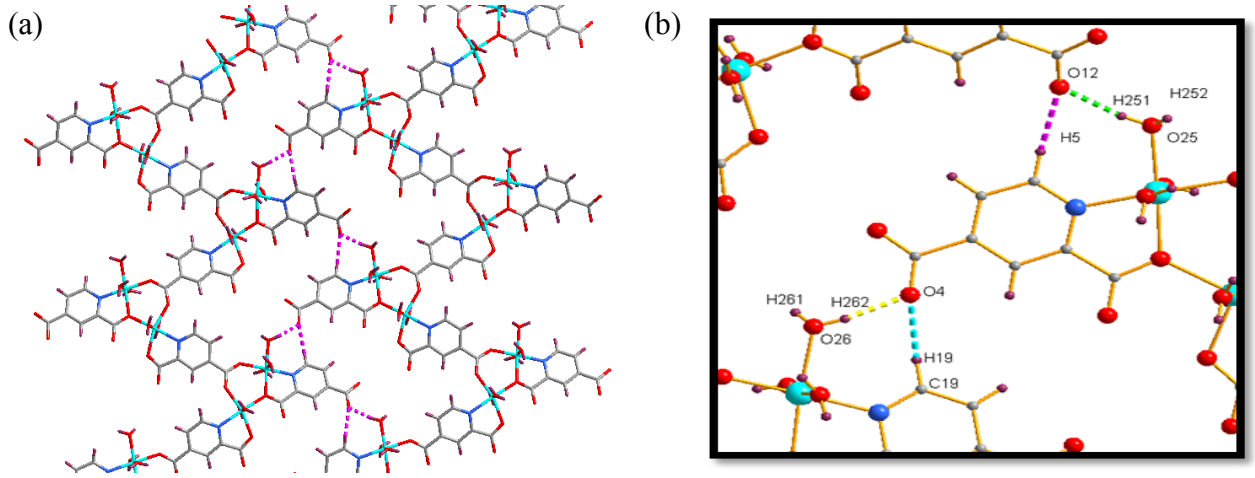

Fig. S4 (a) A view of zigzag chains of **2**, which are hydrogen-bonded into a 2D layer. (b) The hydrogen-bonding interactions occur via O26–H26⋯O4, O25–H26⋯O12, and other weak interactions with C19–H19⋯O4, C5–H5⋯O12.

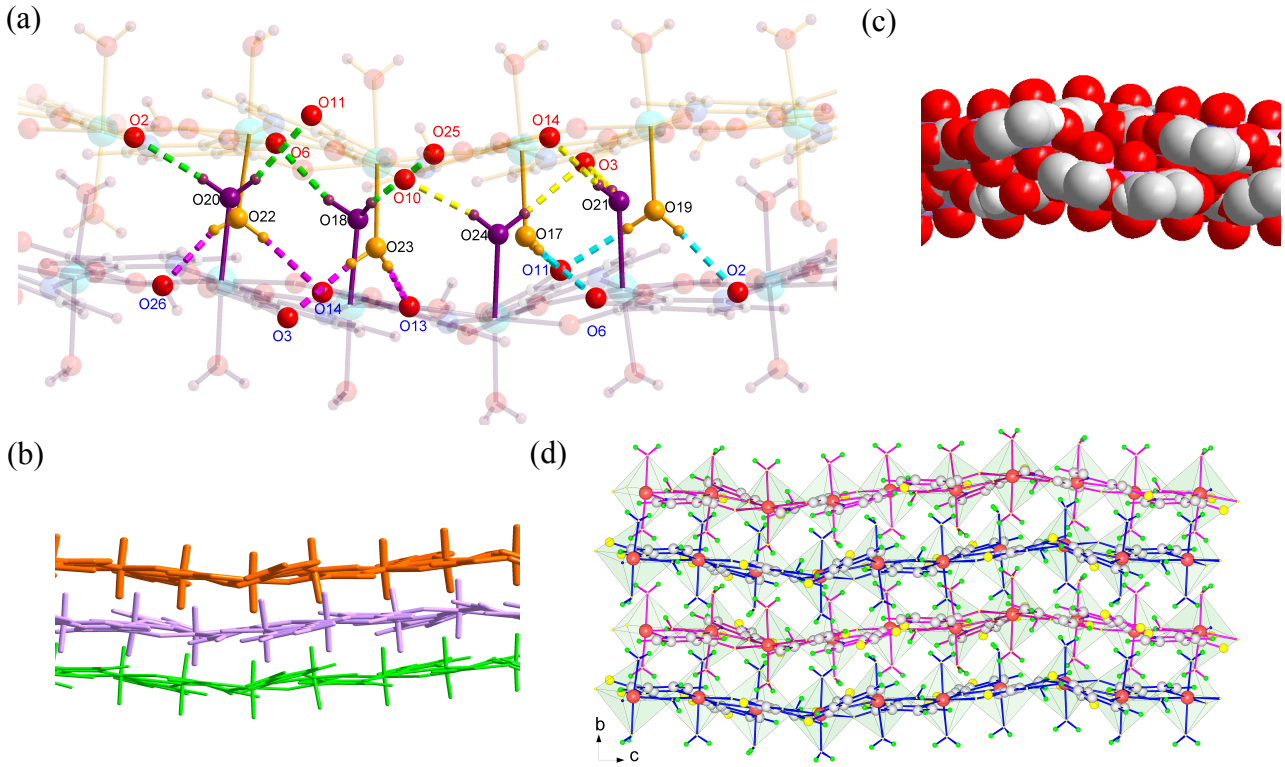

Fig. S5 Structures of **2**: (a) the layers are hydrogen-bonded into a 3D MOF; (b) the layers are stacked in an ABAB manner; (c) the 2D layers reveal in a space-filling mode; (d) the layers present in polyhedral mode.

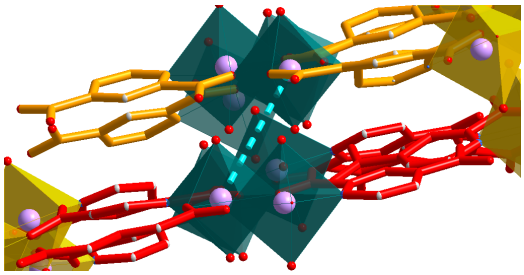

Fig. S6 Polyhedral presentation of the closest layers of **2**, the separation of Co···Co is 5.61 Å in the dotted blue line.

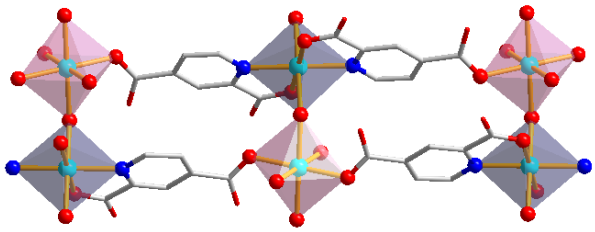

(a)

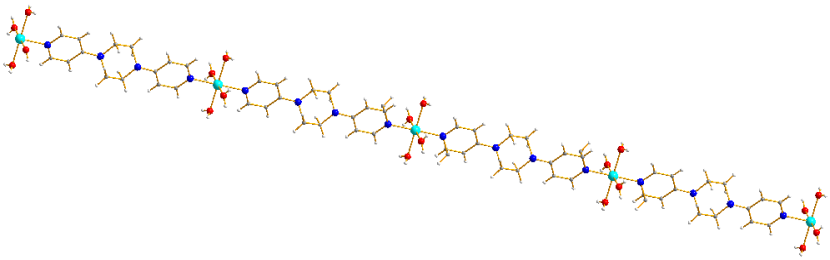

(b)

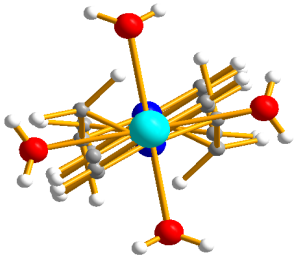

Fig. S7 (a) Ball-and-stick representation of the 1D polymer chain of **3** viewed along the *c* axis; (b) viewed along the *b* axis.

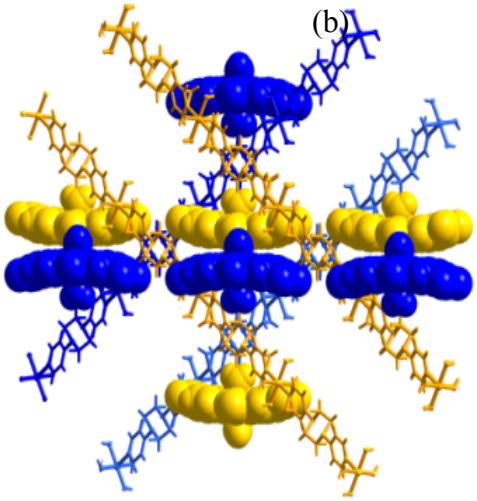

Fig. S8 A pair of discrete anionic species, which are included within each void of **3** in a space-filling model along the *c* axis.

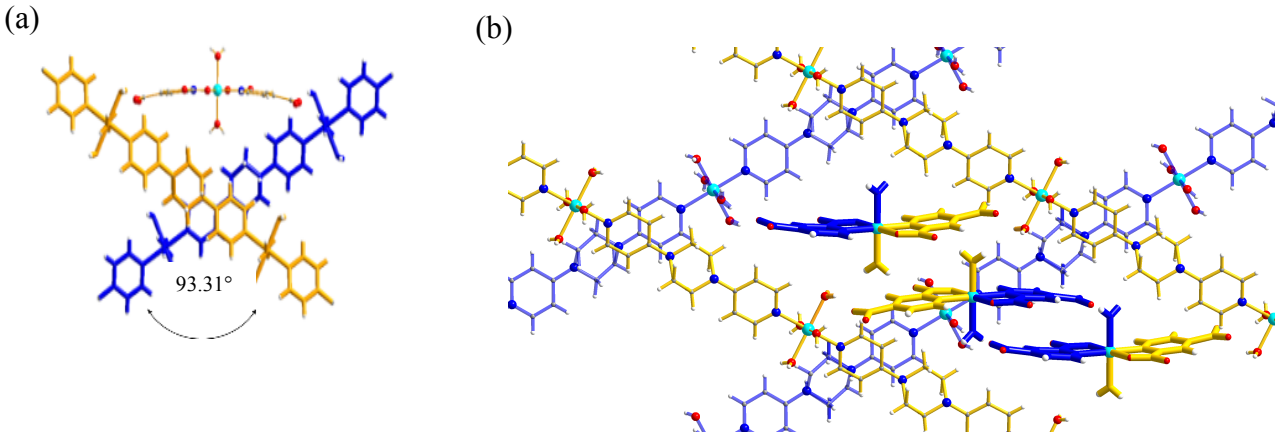

Fig. S9 (a) Two 1D polymer chains are intersected with angle of 93.31°. (b) A grid-type 2D network of **3** is built by the cationic chains $\{[Co(dpyp)(H_2O)_4]^{2+}\}_n$, which are efficiently attracted by the half parts of included anionic complexes $[Co(2,4\text{-pydc})_2(H_2O)_2]^{2-}$ (highlighted in different colors).

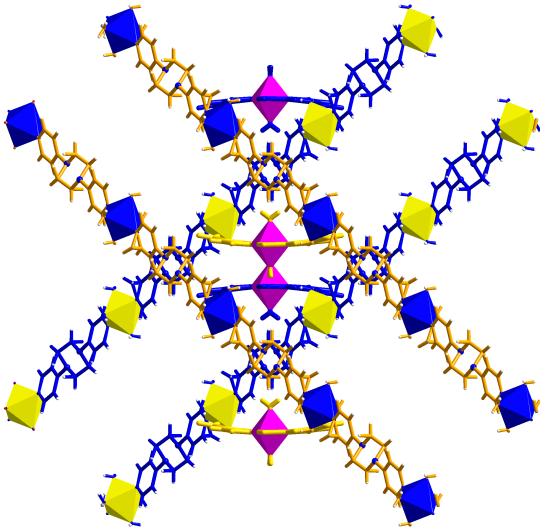

Fig. S10 A grid-type 2D network of **3** that is constructed by the cationic chains $\{[Co(pydp)(H_2O)_4]^{2+}\}_n$ and the included complexes $[Co(2,4\text{-pydc})_2(H_2O)_2]^{2-}$.

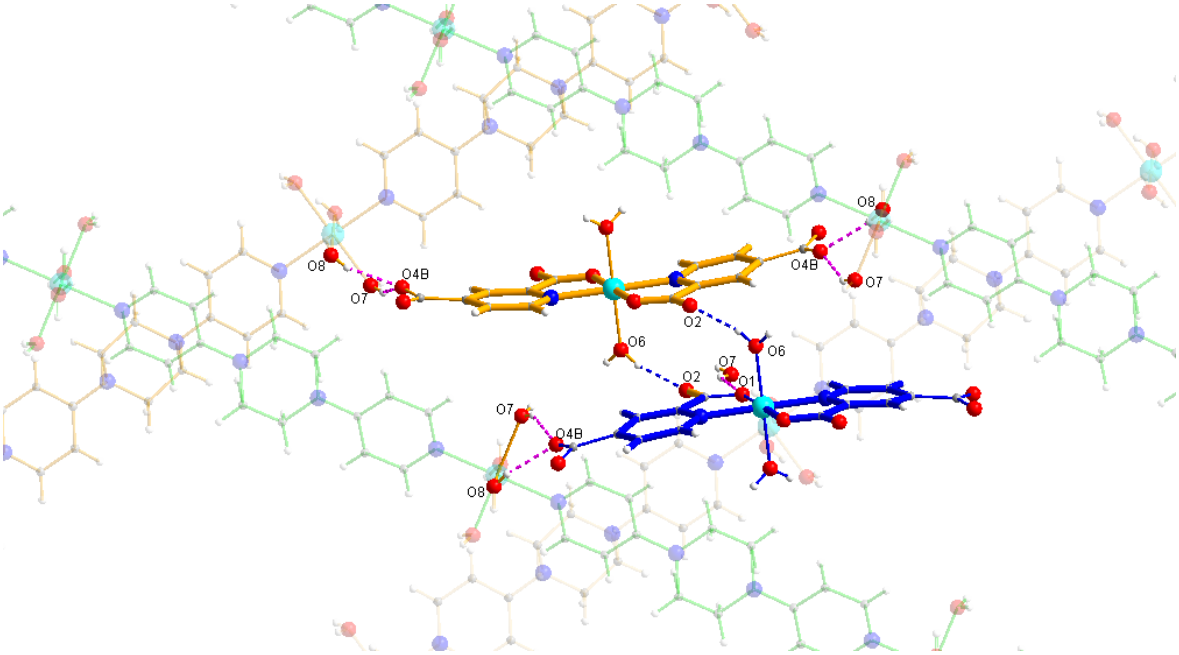

Fig. S11 The cationic chains $\{[Co(pydp)(H_2O)_4]^{2+}\}_n$ are nicely connected with the included molecules $[Co(2,4\text{-pydc})_2(H_2O)_2]^{2-}$ via hydrogen-bonding interactions, which are highlighted in dashed lines.

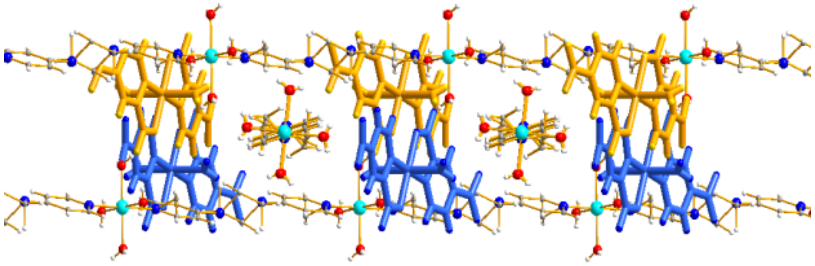

Fig. S12 1D cation chains of $\{[Co(pydp)(H_2O)_4]^{2+}\}_n$ are nicely linked by the anionic complexes $[Co(2,4\text{-pydc})_2(H_2O)_2]^{2-}$, leading to the formation of a 3D framework of **3**.

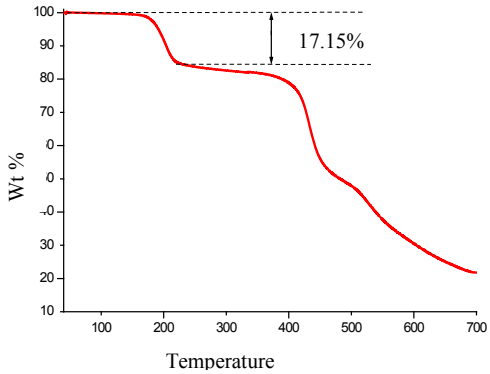

Fig. S13 Thermogravimetric analysis (TGA) curve for **1**.

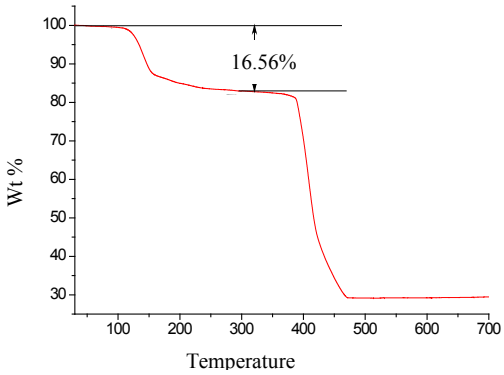

Fig. S14 Thermogravimetric analysis (TGA) curve for **2**.

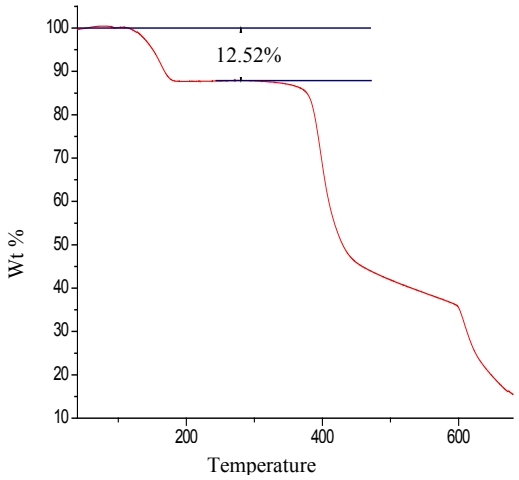

Fig. S15 Thermogravimetric analysis (TGA) curve for **3**.

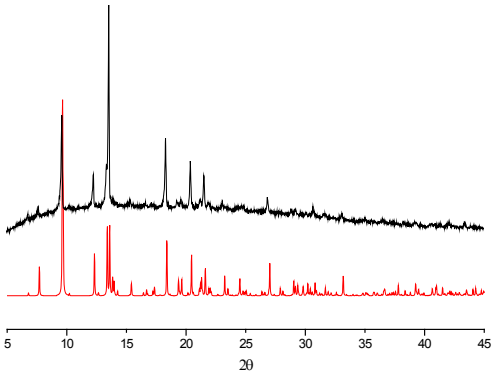

Fig. S16 Powder X-ray diffraction (PXRD) patterns for **1** (as-synthesized, black; simulated, red).

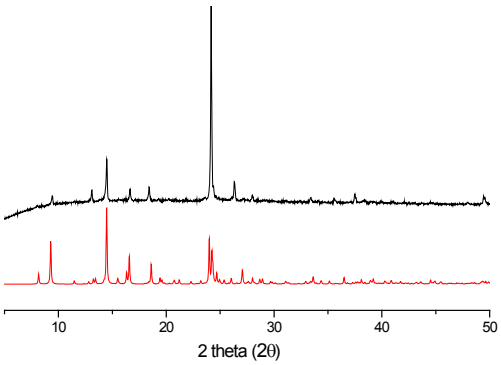

Fig. S17 Powder X-ray diffraction (PXRD) patterns for **2** (as-synthesized, black; simulated, red) .

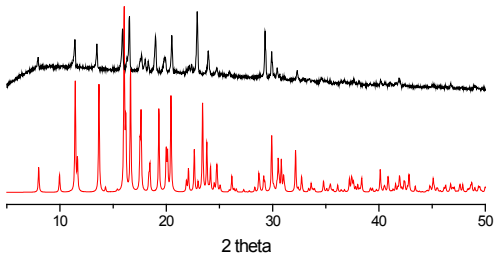

Fig. S18 Powder X-ray diffraction (PXRD) patterns for **3** (as-synthesized, black; simulated, red).

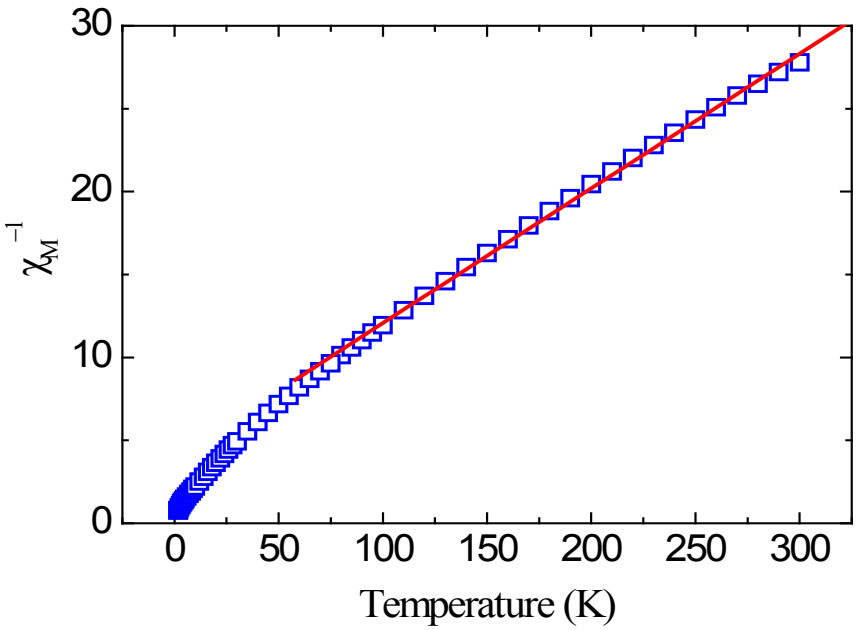

Fig. S19 Plot of χ_M^{-1} vs. T for compound **1**. The solid line is estimated from the Curie–Weiss law.

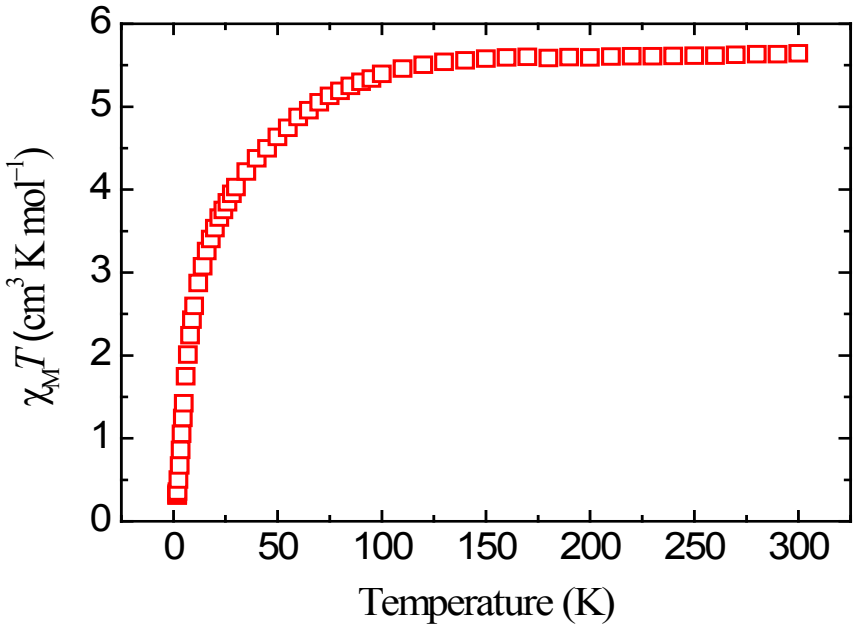

Fig. S20 Plot of χ_MT vs. T for a powder compound **2**.

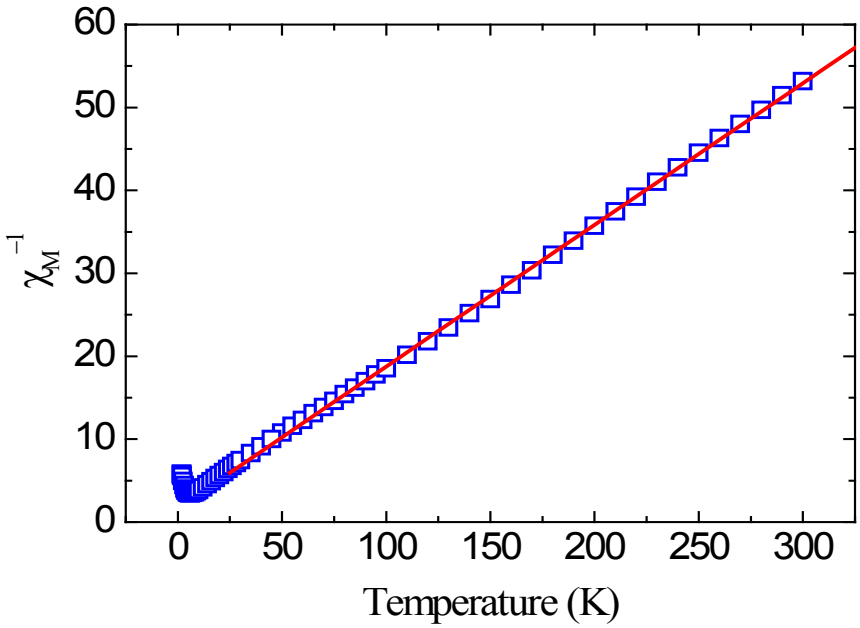

Fig. S21 Plot of χ_M^{-1} vs. *T* for compound **2**. The solid line is estimated from the Curie–Weiss law.

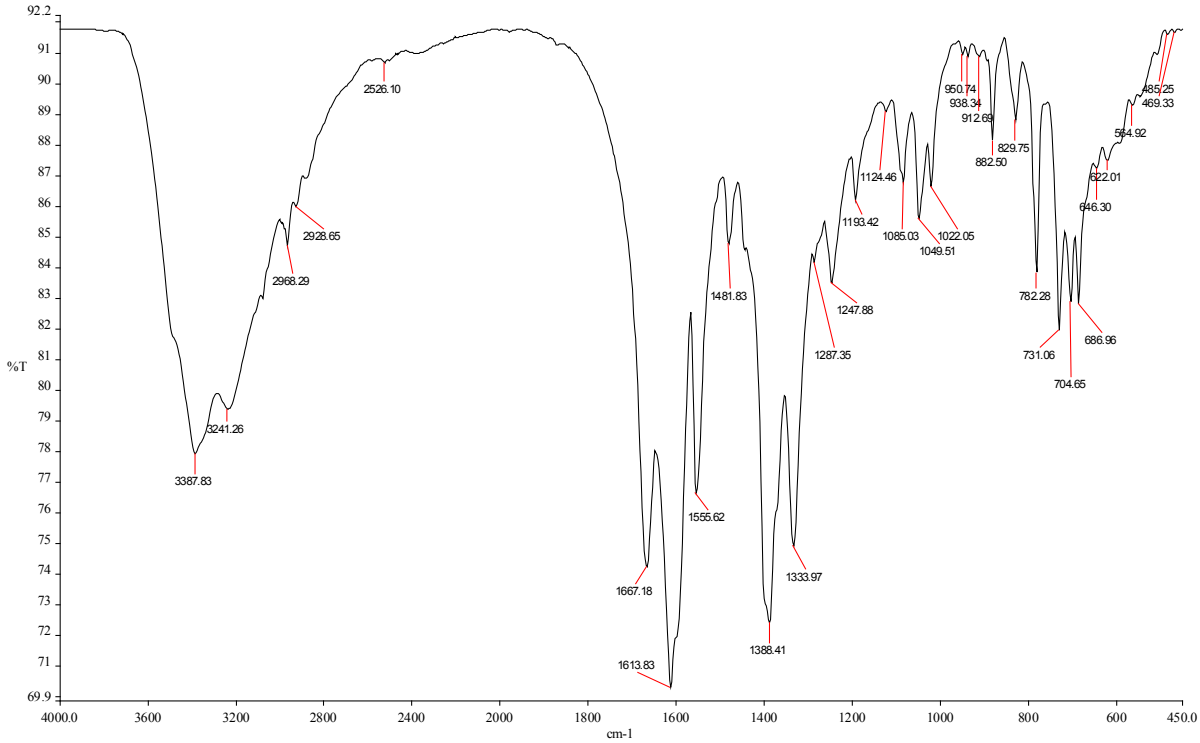

Fig. S22 IR spectrum of **1**.

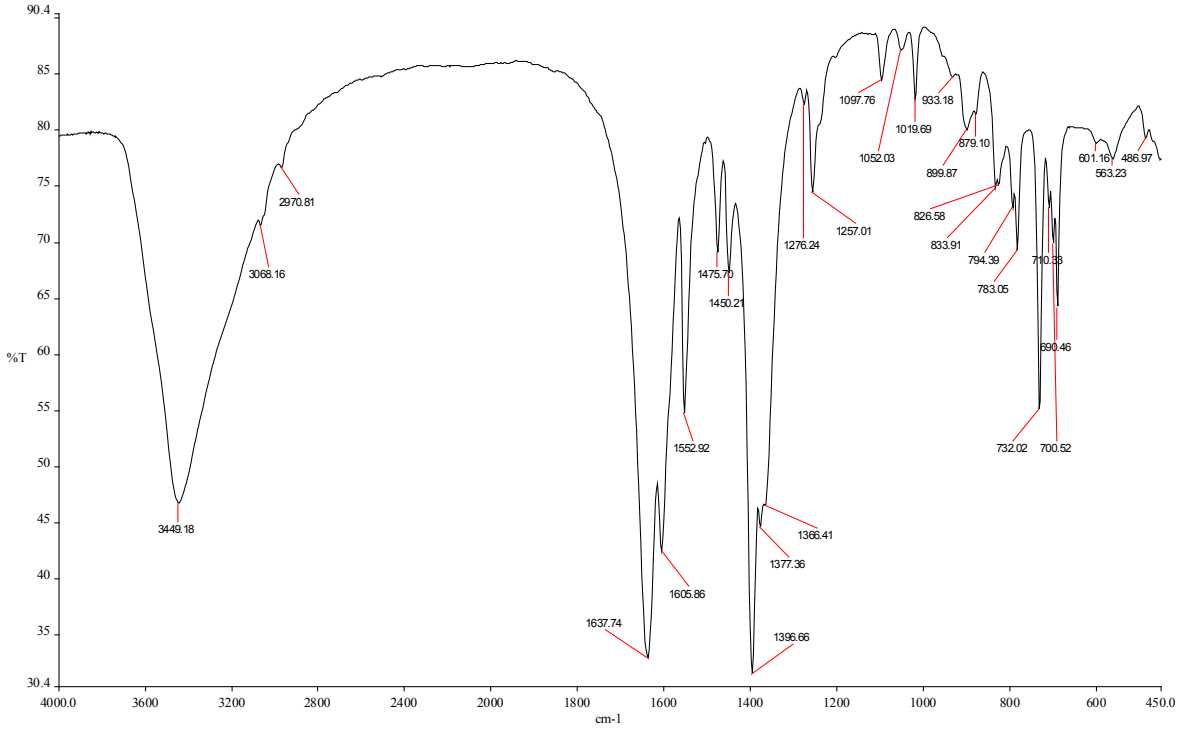

Fig. S23 IR spectrum of **2**.

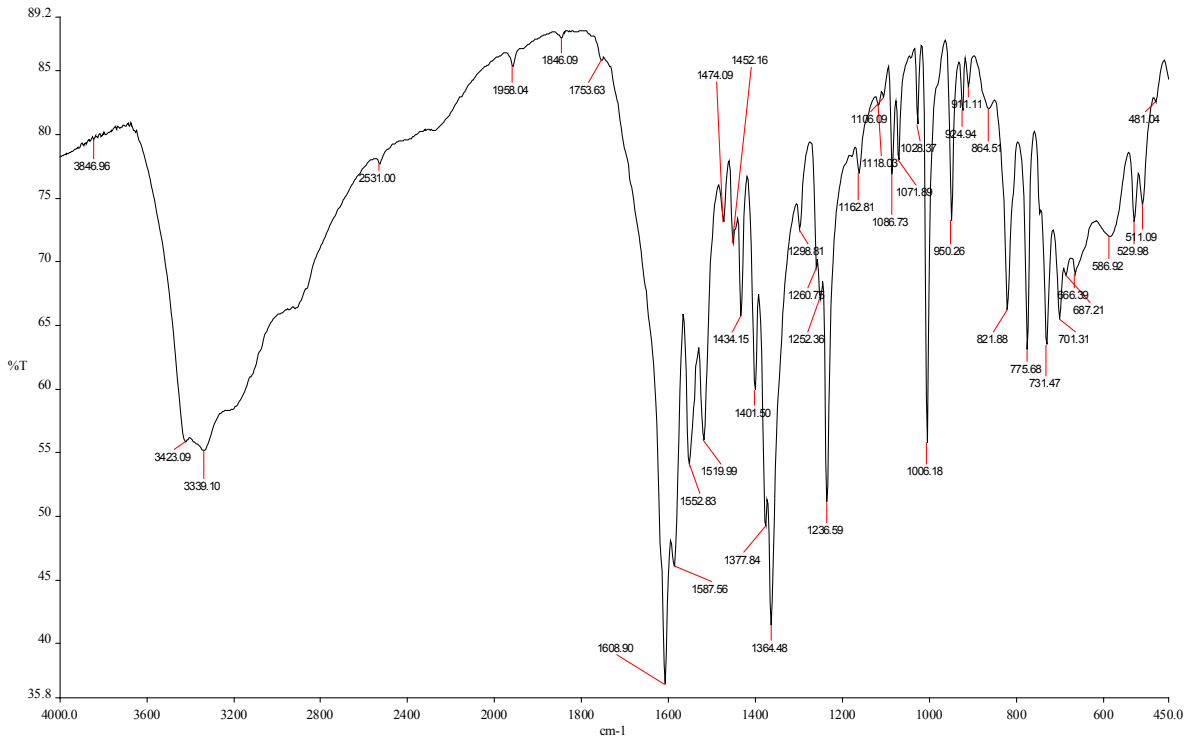

Fig.S24 IR spectrum of **3**.

Table S1 The hydrogen bonding distances (Å) and angles (°) of **1**

D–H···A (Å)	D–H (Å)	H···A (Å)	D···A (Å)	D–H···A (°)
O13–H101···O11	0.88	2.06	2.922(3)	165
O13–H103···O2	0.87	1.83	2.676(3)	165
O14–H103···O1	0.89	1.95	2.825(3)	169

Table S2 The hydrogen bonding distances (Å) and angles (°) of **2**

D–H···A (Å)	D–H (Å)	H···A (Å)	D···A (Å)	D–H···A (°)
O20–H201···O11	0.786	2.173	2.946(4)	167.7
O20–H202···O2	0.799	1.970	2.737(4)	160.7
O18–H181···O25	0.795	2.087	2.815(3)	152.3
O18–H182···O6	0.844	2.012	2.819(3)	159.8
O22–H221···O14	0.789	2.064	2.845(3)	170.4
O22–H222···O26	0.788	2.065	2.822(3)	161.0
O23–H231···O13	0.787	3.284	3.117(3)	70.9
O23–H232···O3	0.802	2.053	2.831(3)	163.3
O21–H211···O14	0.804	1.919	2.716(3)	171.2
O21–H212···O3	0.808	1.847	2.647(3)	170.3
O24–H241···O3	0.823	1.888	2.708(3)	173.1
O24–H242···O10	0.774	1.864	2.614(3)	163.4
O17–H171···O11	0.819	1.828	2.641(3)	172.4
O17–H172···O6	0.663	2.065	2.702(3)	161.7
O19–H192···O2	0.788	2.047	2.807(4)	162.3
O25–H251···O12	0.828	1.790	2.608(3)	168.7
C5–H5···O12	0.950	2.276	3.136(4)	150.2
O26–H262···O4	0.816	3.144	2.822(3)	105.8
C19–H19···O4	0.949	2.322	3.117(4)	140.9

Table S3 The hydrogen bonding distances (Å) and angles (°) of **3**

D–H···A (Å)	D–H (Å)	H···A (Å)	D···A (Å)	D–H···A (°)
O8–H8···O4	0.779	1.863	2.642(3)	164.8
O7—H7···O4	0.803	2.043	2.752(3)	147.6
O6—H6···O2	0.806	1.875	2.675(2)	172.0
O7—H7···O1	0.811	3.035	3.630(3)	132.2